Microwave Resonance in Gadolinium-Iron Garnet Crystals

Abstract: Ferrimagnetic resonance has been observed in single crystals of gadolinium-iron garnet at 9479 and 23,725 mc. The resonance behavior is discussed in terms of a two-sublattice theory. The gadolinium g-factor is equal to 2.006 above -90° C and increases at lower temperatures. The gadolinium ions contribute to the anisotropy below -40° C. The assignment of separate damping constants to each sublattice explains the sharp variation in over-all damping with temperature near the compensation point.

Introduction

Gadolinium-iron garnet is one of a series of ferrimagnetic oxides which were discovered about three years ago.1 These oxides, with the crystal structure of the mineral garnet, have the composition R₃Fe₅O₁₂, where R represents yttrium or one of the rare earths between samarium and lutetium in the periodic table. Pauthenet² has measured the magnetic moments of these oxides and explained their unusual dependence on temperature and applied field in terms of Néel's theory of ferrimagnetism. The magnetizations of gadolinium- and yttrium-iron garnets are shown in Fig. 1. In yttrium-iron garnet, three iron ions per formula unit are each surrounded by tetrahedra of oxygen ions, while two iron ions are surrounded by octahedra of oxygen ions. The magnetization of yttrium garnet is due to antiparallel coupling between these two groups, or sublattices, of iron ions.^{2,3} In gadolinium garnet, there is an additional, much weaker coupling which aligns the moments of the gadolinium ions antiparallel to the resultant moment of the iron ions.

Microwave-resonance experiments furnish a useful tool for investigating these phenomena. A typical experiment consists in observing the absorption of microwave energy by a small piece of magnetic material placed in a variable magnetic field. When the applied magnetic field is such that, in combination with internal crystalline fields, it yields a frequency of gyromagnetic precession equal to the applied microwave frequency, resonant absorption of energy takes place. Since the internal fields give rise to terms dependent on the angles between the applied field and the crystallographic axes, these effects can be separated from those arising from the applied field. The

angular variation in resonant field measures the crystalline anisotropy; the proportionality constant between total effective field and frequency measures the gyromagnetic ratio; the width of the resonance measures the damping of the motion of the magnetization. Detailed analysis further shows that the g-factors of the individual sublattices to some extent can be determined separately, particularly in connection with the interpretation of the resonance behavior near a compensation point: i.e., a temperature at which the sublattices have equal and opposite magnetization, with a net zero total magnetization.

Yttrium-iron garnet is the simplest one of these oxides to understand, since the yttrium ion has no magnetic moment. It also is of considerable technical interest because of the very small damping, i.e., narrow line width, and has been studied by several authors.^{4,5,6} Among the rare-earth ions with a magnetic moment, the behavior of Gd³⁺ should be the easiest to interpret, since its moment is due only to electron spins.

Microwave resonance absorption has been investigated in polycrystalline samples of gadolinium-iron garnet. Analysis of these measurements gives a value for the difference in the g-factors of the iron and gadolinium ions $g_{\rm Fe}$ - $g_{\rm Gd}$ =0.010, in good agreement with our single-crystal measurements. These polycrystalline measurements do not give quantitative information about the anisotropy and also cannot be unambiguously interpreted in the vicinity of the compensation point. A preliminary report on some of the present single-crystal results has been given elsewhere.

In the subsequent developments the terms g-factor and

gyromagnetic ratio (γ) are both used as measures of the proportionality between resonance frequency and magnetic field. They are related by

$$\gamma = \frac{2\pi g\beta}{h}$$

where β is the Bohr magnetron and h is Planck's constant. For a free electron spin g=2.0023 and $\gamma/2\pi=2.8$ megacycles per oersted.

Experimental apparatus and results

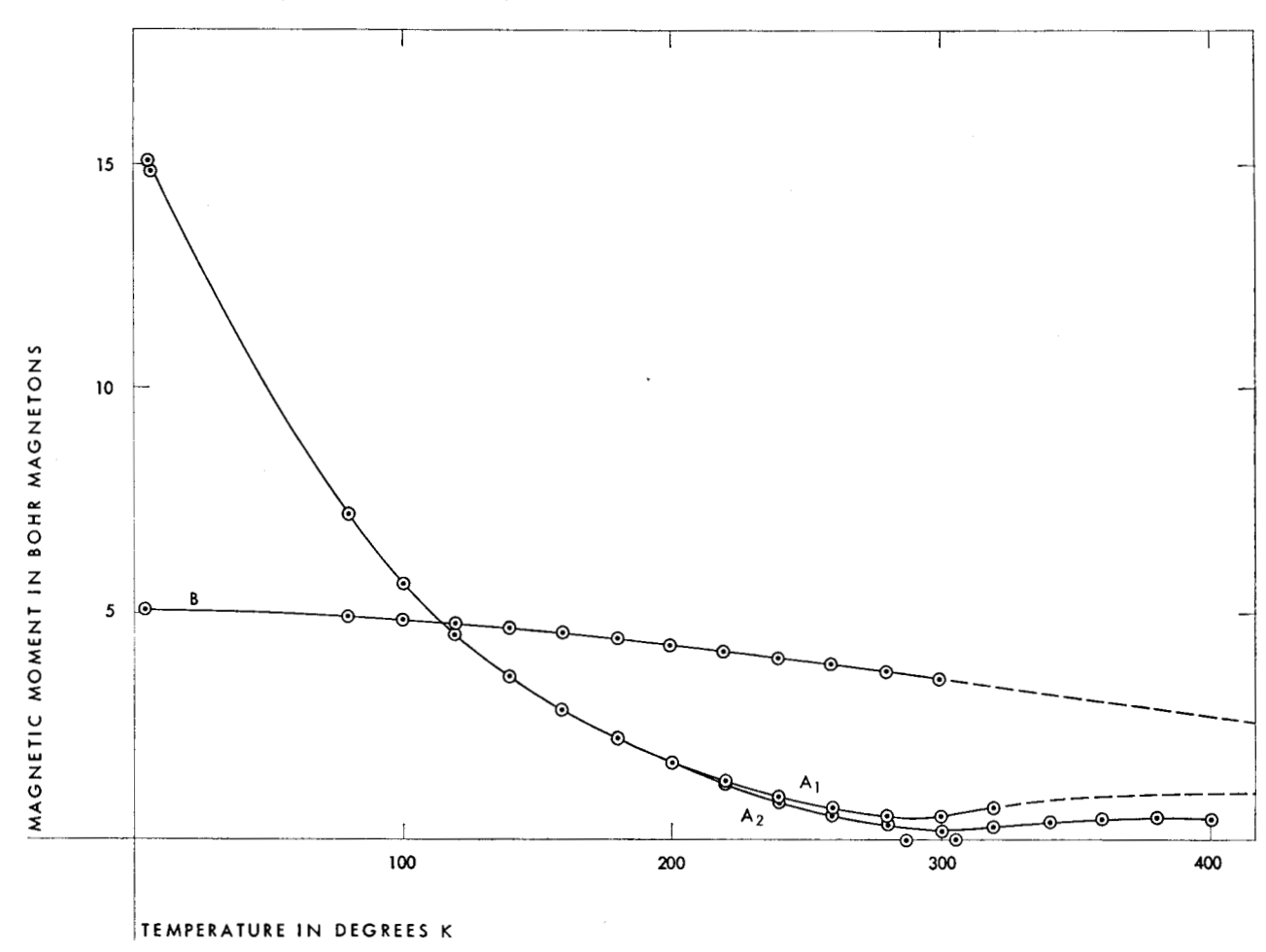
Since these garnet compounds melt incongruently in an air or oxygen atmosphere, the conventional methods of growing crystals from the liquid of the same composition could not be used. A mixture of iron and gadolinium oxides (80 mol % Fe_2O_3 , 20 mol % Gd_2O_3) was heated to $1520\,^{\circ}$ C in oxygen and then slowly cooled. During cooling, the garnet crystallizes from the iron oxide liquid. The resulting crystals were small, about 1 mm in linear dimensions, and were difficult to remove from the iron oxide. Concentrated hydrochloric acid was used to free the crystals and, in the course of this treatment, it became

apparent that many of the crystals were "skeletons" with inclusions of iron oxide. Sound crystals were ground to spheres of approximately 0.020" diameter and examined microscopically and by x-rays for evidence of inclusions. Although no evidence of inclusions was found in the samples used for the resonance measurements, a weak absorption peak was observed near the compensation temperature, which appeared to be due to small amounts of an impurity.

Magnetization measurements were made on these crystals, using an apparatus similar to that described by Maxwell and Pickart.¹⁰ The results are shown in Fig. 1 together with the magnetization of yttrium garnet crystals prepared by the same method.

Cylindrical transmission cavities operating in the TE_{011} mode were used at both X and K bands. At X band, the sample was cemented to a 1/8" diameter copper post mounted axially in the cavity; temperatures other than room temperature were obtained by heating or cooling the copper post. The tip of the post was tapered to minimize rf field distortion near the sample. A copper-constantan thermocouple, running coaxially through the post

Figure 1 Magnetizations of gadolinium- and yttrium-iron garnets versus temperature. A_1 and A_2 :Gd, H_a =4×10³ oe; B:Y, H_a =7×10³ oe.



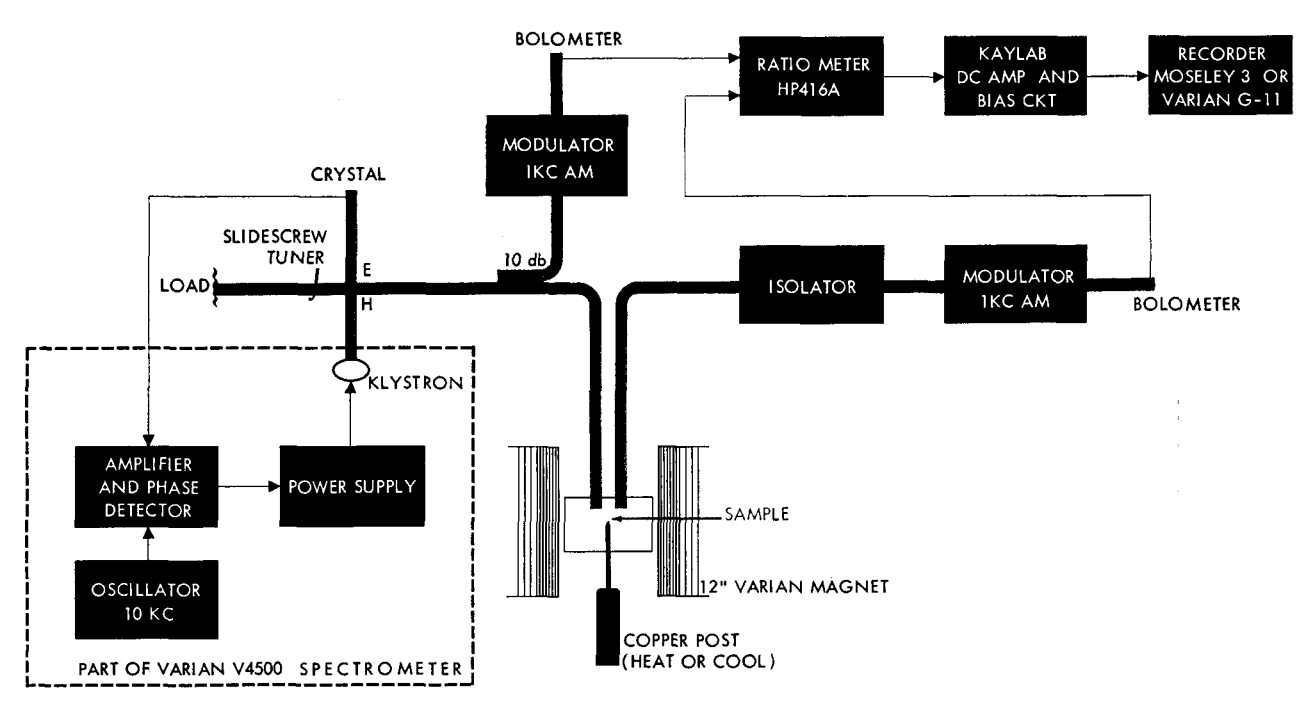


Figure 2 Block diagram of the ferrimagnetic resonance spectrometer used at X-band.

and soldered at the sample location, was used to monitor temperature. The resonant frequency was 9479 Mc. For the K-band measurements the sample was cemented on an axial quartz post and temperature changes accomplished by immersing the cavity in a constant-temperature bath. Condensation in the cavity and waveguide was prevented by flushing and pressurizing with helium at the start of each run. The resonant frequency of this cavity at room temperature was 23,725 Mc. Other cavities and other cooling arrangements, including immersion of the cavity in liquid helium or liquid nitrogen, were used in some comparison experiments.

The spectrometer used at X-band is shown in Fig. 2. Auxiliary components such as attenuators, wavemeter, et cetera, are not shown. The klystron was frequency-stabilized on the sample cavity for all X-band measurements; the system actually used is part of the Varian V 4500 spectrometer used for paramagnetic resonance in this laboratory. A 10-kc oscillator frequency modulates the klystron so as to sweep a small portion of the cavity resonance. The signal reflected by the cavity is amplified, phase detected, and applied to the klystron reflector to compensate for frequency drifts.

A measurement of the power absorbed by the sample was obtained by using a Hewlett-Packard 416A ratio meter to measure the power-transmission coefficient ($T=P_{\rm transmitted}/P_{\rm incident}$) of the cavity as described by White and Solt.¹¹ The power absorbed in the sample, P_a , is given by:

$$P_{a} = \frac{1}{Q_{L}^{e}} \left[\left(\frac{T_{0}^{e}}{T} \right)^{1/2} - 1 \right], \tag{1}$$

where Q_L^e is the loaded Q of the empty cavity, T_0^e the power-transmission coefficient of the empty cavity, and T is the power-transmission coefficient of the cavity containing the sample.

For the K-band experiments, the klystron was swept across a mode with a 100-cycle sawtooth signal. The power output of the cavity was peak-detected, amplified, and applied to the recorder Y-axis.

The relative magnetic field was measured either by a Rawson Model 722 rotating flip coil or by time scanning the magnet current linearly. A proton probe was used for accurate calibration of the scan. Reduction to absolute field was facilitated by use of a small amount of dpph (diphenyl-picryl hydrazyl, g=2.0036) near the sample.

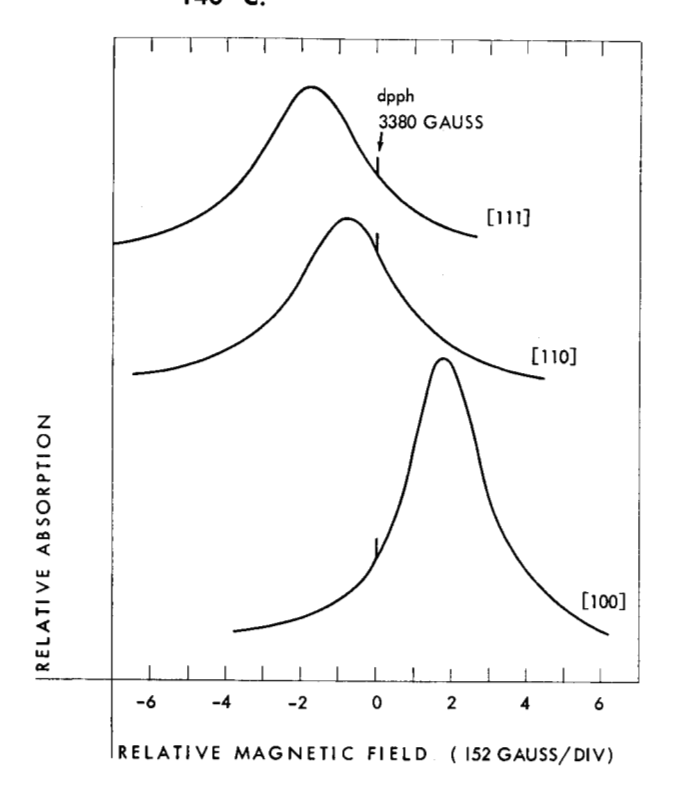
The plots of absorbed microwave power as a function of magnetic field are obtained by semi-automatic recording techniques. Typical curves are shown in Figs. 3 and 4 for the three principal crystallographic directions, [100], [110] and [111]. These resonances are symmetrical, strong and well-defined at temperatures 50° or more from compensation point (Fig. 3). As the compensation point is approached, the resonances become weaker, broader and in some cases asymmetric, as shown in Fig. 4. Close to the compensation temperature, a weak extra resonance appears at low fields (Fig. 4). This resonance was observed in both X- and K-band measurements and may be present, but masked by the larger absorption, at temperatures farther from the compensation point. From the relative independence of this resonance on crystal orientation and temperature, it is thought to be due to small inclusions (of the order of 1% of the volume of the sample) of a magnetic iron oxide in the crystals.

An individual absorption curve is characterized by the field H_{τ} at which maximum absorption occurs and by the difference $2\Delta H$ between the two fields at which the absorption is one-half of its maximum value. Fig. 5 shows the variation in H_{τ} for the magnetic field applied along different directions in the (110) plane of the crystal. The temperature dependence of H_{τ} for the three principal crystallographic directions is shown in Fig. 6. The widths of the resonance in the three directions are shown in Fig. 7.

Discussion

Magnetization measurements on the garnets show that the moments of the rare-earth ions are much more weakly coupled than are the iron moments. In discussing the resonance behavior of gadolinium-iron garnet, we assume that the two iron sublattices can be treated as a unit. Because of the weak interaction with the gadolinium-ion moments, the magnetization of the iron sublattice will be essentially equal to the magnetization of vttrium-iron garnet. Since the "molecular field" acting on the gadolinium moments is so weak, the magnetization of the gadolinium lattice exhibits a susceptibility practically equal to the usual paramagnetic susceptibility of Gd3+ ions. Although this dependence of the gadolinium magnetization on the external field modifies the resonance conditions in the immediate neighborhood of the compensation temperature, 12 it has little effect in the temperature range of our data (Fig. 6) and we will neglect it.

Figure 3 Absorption curves for the three principal crystallographic directions at 9479 mc, —140° C.



The theory of ferrimagnetic resonance in systems of two coupled sublattices has been extensively treated in the literature^{13,14} but with two exceptions^{9,15} the effects of damping have been neglected. To provide a basis for consideration of the marked increase of the line widths observed around the compensation point, we will include a damping term in the initial equations for the motion of the sublattice magnetizations. For our purpose, it is more convenient to use an equation proposed by Gilbert¹⁶ instead of the more familiar Landau-Lifshitz equation. We write an equation

$$\frac{d\mathbf{M}_{i}}{dt} = \gamma_{i}(\mathbf{M}_{i} \times \mathbf{H}_{i}) - \frac{\alpha_{i}}{|\mathbf{M}_{i}|} \left(\mathbf{M}_{i} \times \frac{d\mathbf{M}_{i}}{dt}\right)$$
(2)

for each sublattice. \mathbf{M}_i represents the magnetization, γ_i the gyromagnetic ratio and α_i the damping parameter of the i^{th} sublattice. The quantity \mathbf{H}_i includes not only the applied fields but also terms representing exchange, anisotropy and demagnetizing effects. These effects have been considered extensively¹⁴ and, for the present, we neglect anisotropy and demagnetizing effects. The method of solving Eq. (2) for two coupled sublattices is well known but very laborious. Fortunately, for our present purpose, we do not need to solve these equations. We wish to know whether the motion of the net magnetization $\mathbf{M} = \mathbf{M}_1 + \mathbf{M}_2$ can be described by an equation similar to Eq. (2). We assume that the solution of Eq. (2) will have the form

$$\frac{d\mathbf{M}_i}{dt} = \mathbf{\omega} \times \mathbf{M}_i \,, \tag{3}$$

where, because of the strong exchange coupling between the sublattice magnetizations, the angular velocity ω is the same for both sublattices. Substituting this into Eq. (2) and introducing the angular momenta $\mathbf{S}_i = \mathbf{M}_i/\gamma_i$, we obtain

$$\frac{\boldsymbol{\omega} = \mathbf{M}_{1}}{\gamma_{1}} = \mathbf{M}_{1} \times (H_{0} + \lambda \mathbf{M}_{2}) - \frac{\alpha_{1}}{|\mathbf{S}_{1}|} (\mathbf{S}_{1} \times \boldsymbol{\omega} \times \mathbf{S}_{1})$$

$$\frac{\boldsymbol{\omega} \times \mathbf{M}_{2}}{\gamma_{2}} = \mathbf{M}_{2} \times (H_{0} + \lambda \mathbf{M}_{1}) - \frac{\alpha_{2}}{|\mathbf{S}_{2}|} (\mathbf{S}_{2} \times \boldsymbol{\omega} \times \mathbf{S}_{2}) \quad (4)$$

The field has been written to show explicitly the external fields \mathbf{H}_0 and the exchange terms $\lambda \mathbf{M}_i$. We now add the two equations (4), noting that the exchange terms cancel. If, furthermore, the magnetizations are antiparallel, we obtain

$$\frac{\boldsymbol{\omega} \times \mathbf{M}}{\gamma_e} = \mathbf{M} \times H_0 - \frac{\alpha_e}{|\mathbf{S}|} (\mathbf{S} \times \boldsymbol{\omega} \times \mathbf{S}),$$

where γ_e is defined by the equation

$$\mathbf{M}_1 + \mathbf{M}_2 = \gamma_e(\mathbf{S}_1 + \mathbf{S}_2) = \gamma_e[(\mathbf{M}_1/\gamma_1) + (\mathbf{M}_2/\gamma_2)]$$
 (5)

and

$$\alpha_e = \left[\alpha_1 |\mathbf{S}_1| + \alpha_2 |\mathbf{S}_2|\right] / |\mathbf{S}|. \tag{6}$$

This expression for the "effective damping parameter" should be valid under the same conditions as those for which the resonance field is given by an effective gyro-

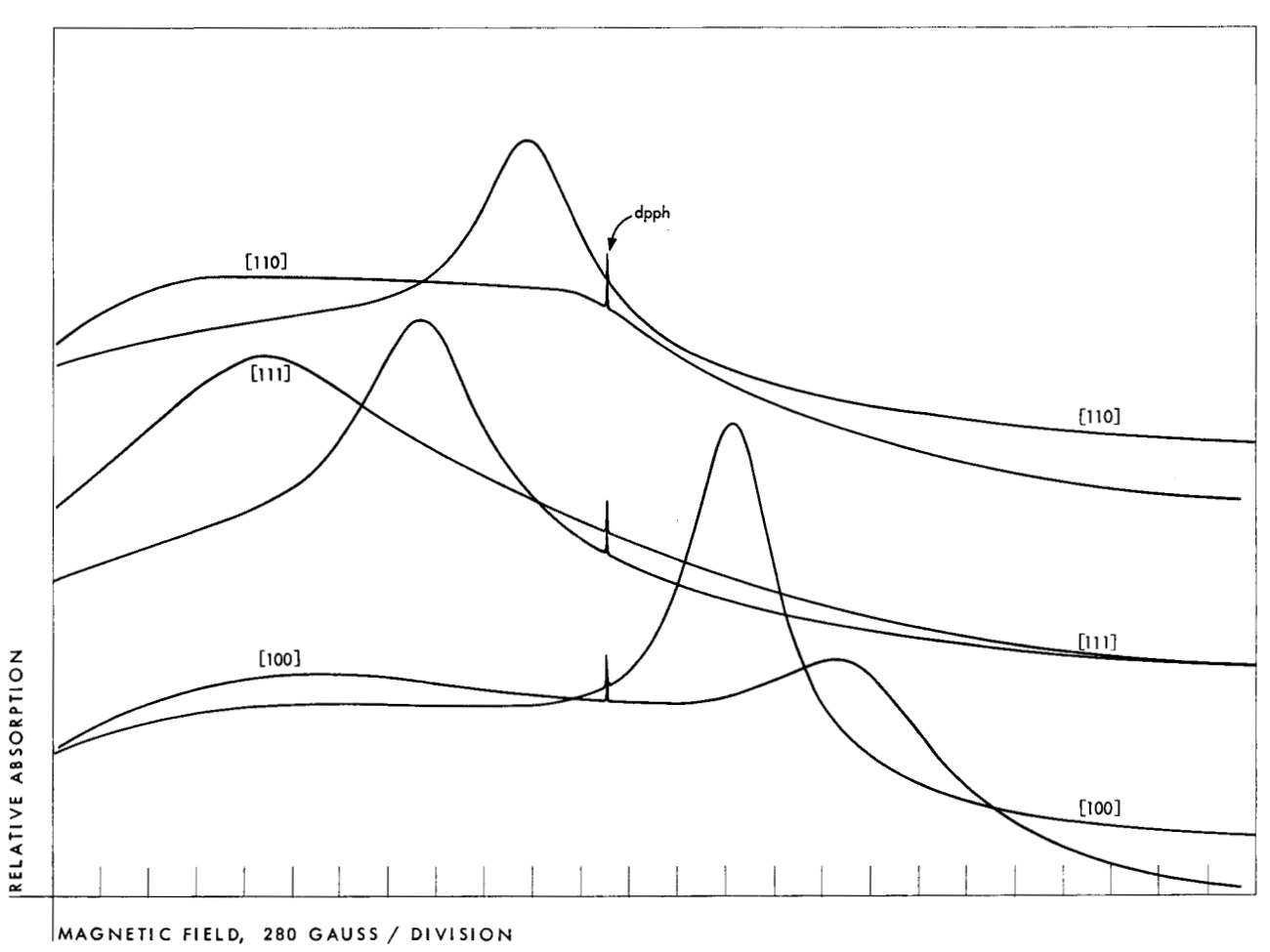
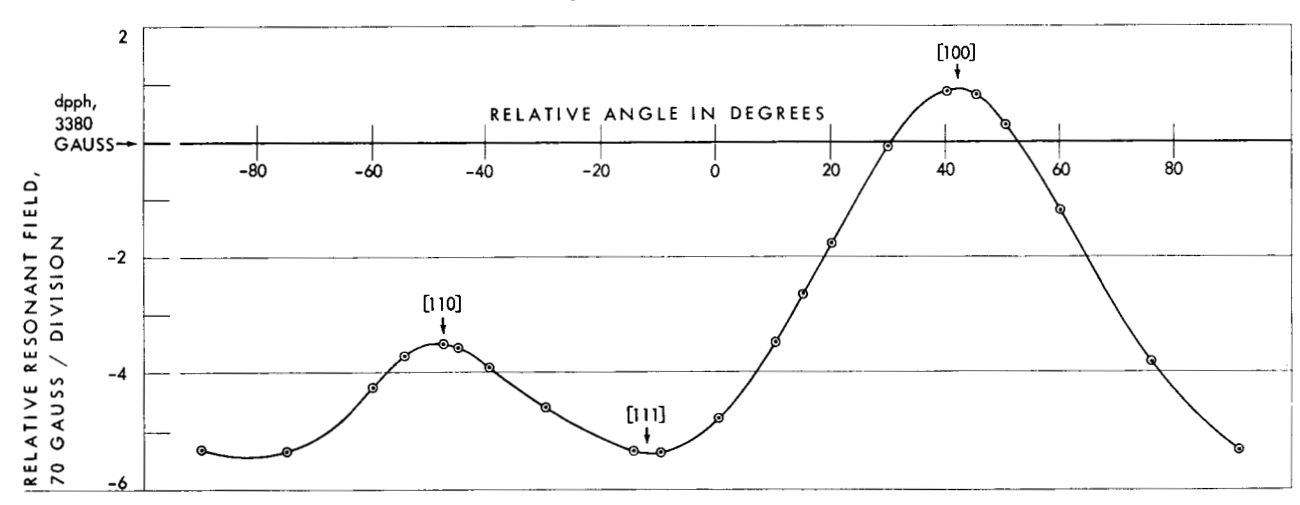


Figure 4 Absorption curves at 9479 mc: in blue, 39° C; in black, 24° C. The extra low field absorption at 24° C is attributed to some impurity (see text).





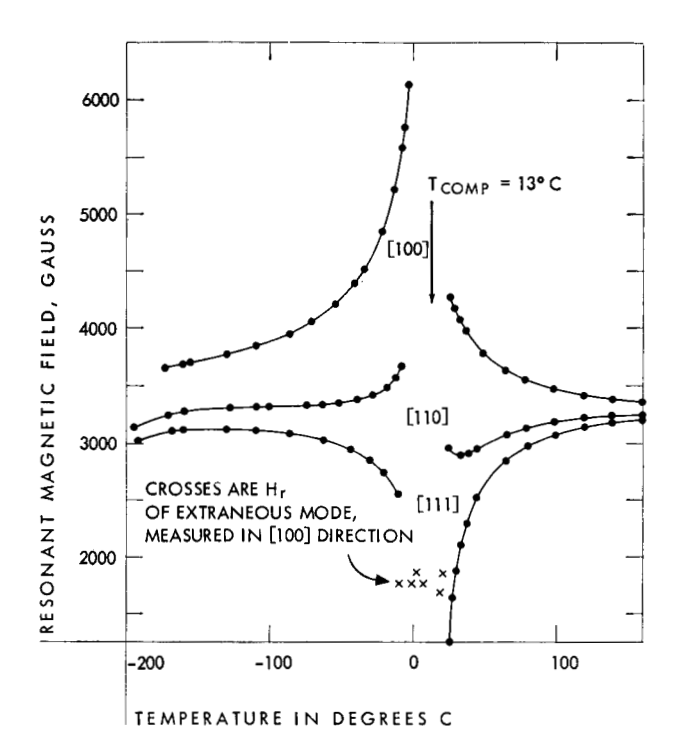


Figure 6 Temperature dependence of resonant field for 21-mil sphere at 9479 mc in the three principal directions.

magnetic ratio. Wangsness¹⁵ has recently obtained an expression for the effective damping parameter by a solution of the equations of motion using a Landau-Lifshitz damping term. He has shown that it is necessary that the equations of motion used for the sublattice magnetizations describe relaxation toward the instantaneous values of the total fields acting on the individual sublattices. An advantage of using the Gilbert equation is that this condition is automatically satisfied.

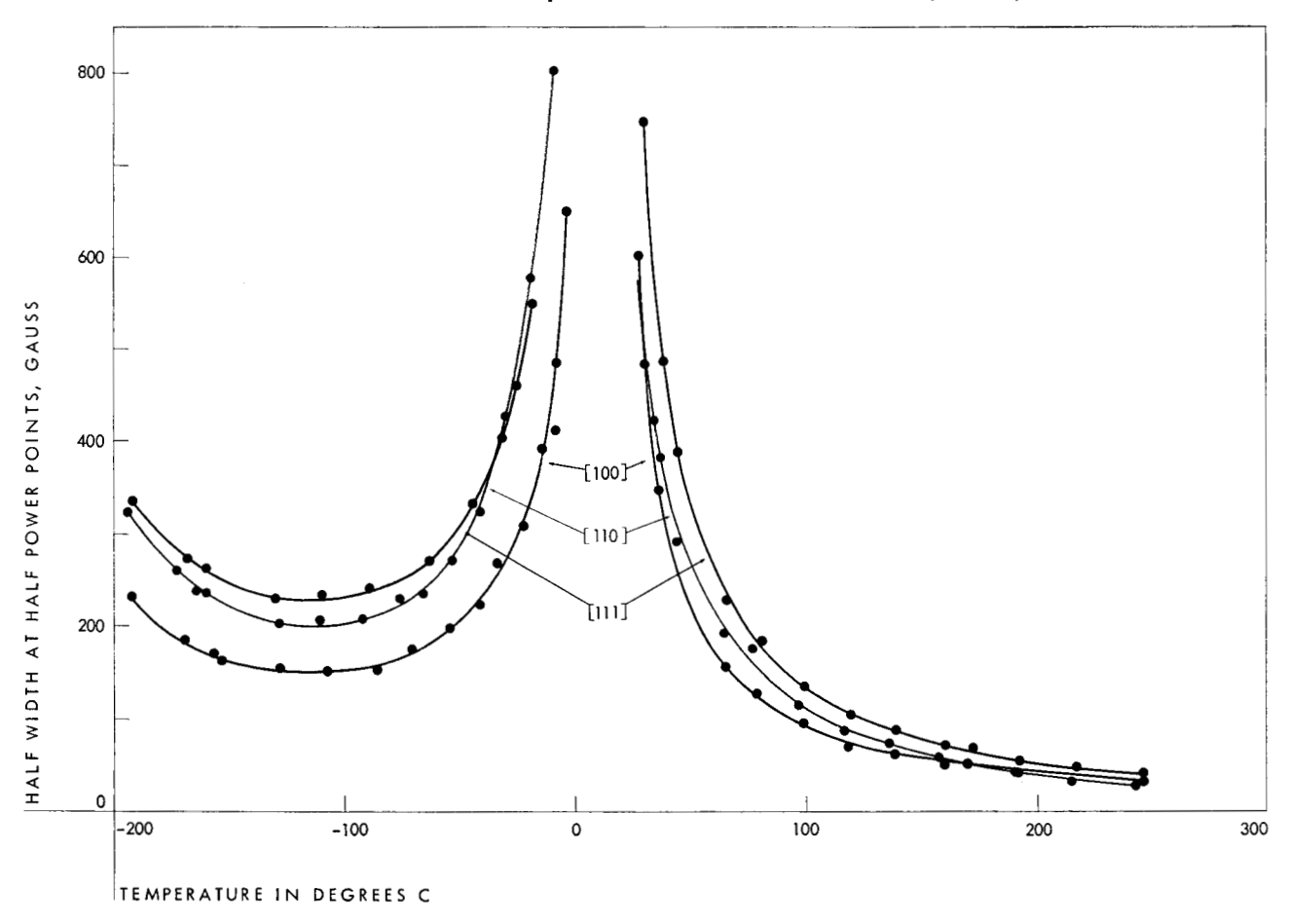
The damping parameter is related to the width of the resonance line by the equation

$$\alpha = \gamma \Delta H/\omega_r$$
, (7)

where $\gamma \Delta H$ is the difference in magnetic fields between the points of half-maximum absorption and ω_r is the resonant frequency. Substituting for α_e and γ_e from Eq. (5) and (6), we obtain

$$|M|\Delta H = \omega_r(\alpha_1|S_1|+\alpha_2|S_2|). \tag{8}$$

Figure 7 Variation of the line width with temperature at 9479 mc for the [100], [110], and [111] directions.



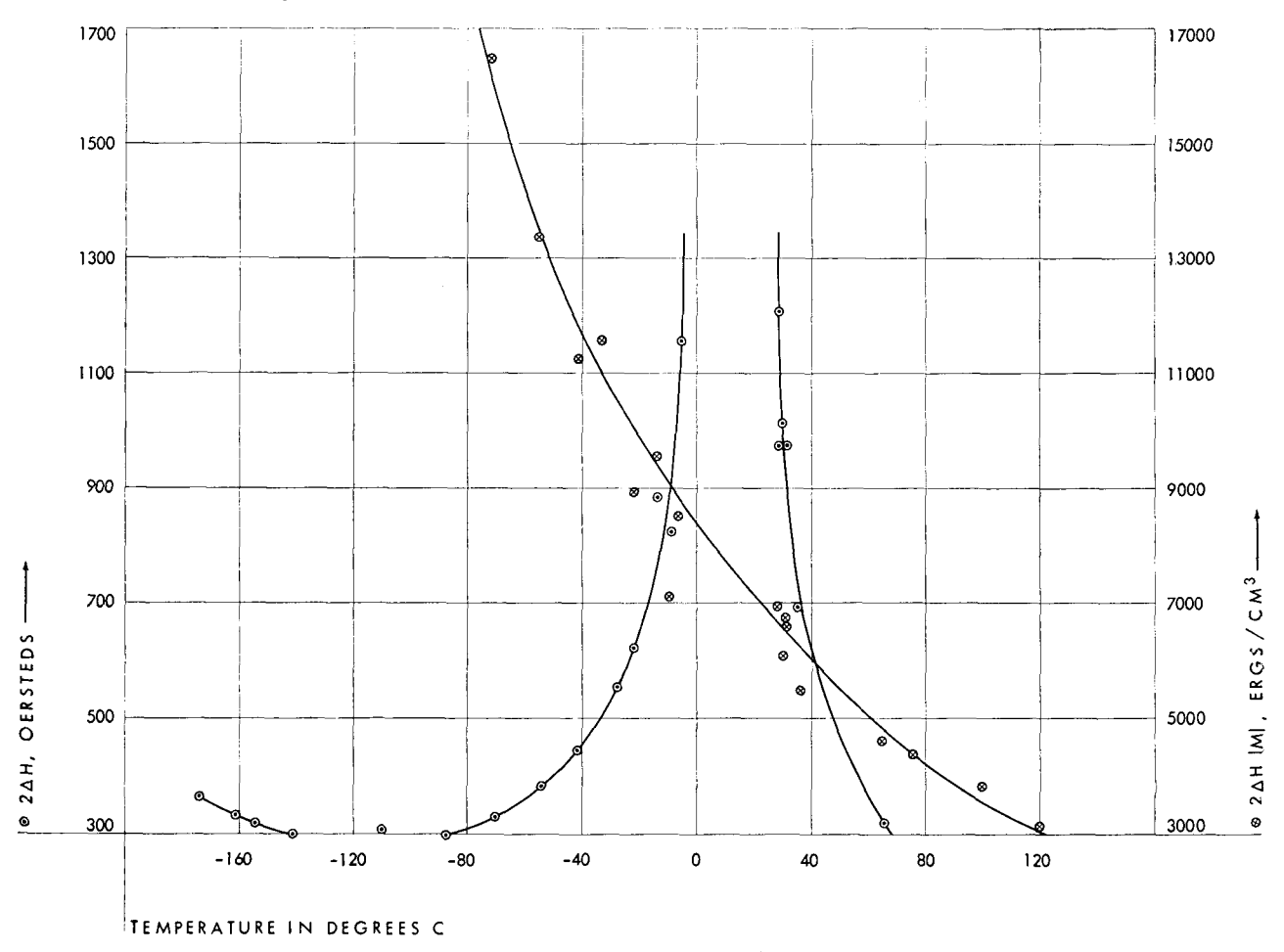
As shown in Fig. 8, the temperature variation of the product $M\Delta H$ agrees qualitatively with Eq. (8). Our measurements, particularly at K-band, and the measurements of Geschwind et al12 show that the line width remains finite at the compensation point. This failure of Eq. (6) to represent the data in the immediate vicinity of the compensation point is understandable from the assumptions involved in its derivation. We have estimated the relative contributions of the iron and gadolinium sublattices to the total damping at room temperature. A value $\alpha_{\rm Fe}$ = 0.002 was obtained from the line width at room temperature in vttrium-iron garnet crystals. At room temperature, our line width for yttrium garnet is in good agreement with data reported by Dillon4 but much narrower lines have been reported.⁶ A value α_{Gd} =0.006 was calculated from the data in Fig. 8. The gadolinium ions contribute much more to the total loss than do the iron ions. This is probably true to an even greater extent for the other rare-earth ions¹⁷ with non-vanishing orbital angular momentum, and hence a stronger coupling to the lattice via spin-orbit interactions.

The dependence of the damping on crystal orientation and frequency is of interest. It is clear from Eq. (7) that,

if α is a scalar parameter, the line width should be independent of orientation. Empirically, the rather large observed variation of line width with crystal orientation might be accounted for by making α depend on orientation. The significance of such a procedure is not clear and we have simply used the narrowest lines, i.e., those in the [100] direction, to calculate values of α . In both gadolinium- and yttrium-iron garnet, the line width appears to be proportional to frequency, i.e., the damping parameter is constant, between 9000 and 24,000 Mc. There is evidence that at lower frequencies (2000 to 3000 Mc) the damping in garnets begins to increase.

We turn now to a consideration of the gyromagnetic ratios of the iron and gadolinium sublattices. In using Eq. (5) to obtain the sublattice γ 's, we need one assumption in addition to the sublattice magnetizations. We assumed that $\gamma_{\rm Fe}$ was equal to the value measured in yttrium-iron garnet, $g_{\rm Fe}=2.020$, and was independent of temperature. We obtain the values of $g_{\rm Gd}$ shown in Fig. 9. Near the compensation point, the calculated values of g_e are quite sensitive to the difference, $g_{\rm Fe}-g_{\rm Gd}$, and relatively insensitive to the individual g values. Our value for this difference, $g_{\rm Fe}-g_{\rm Gd}=0.014$, is in good agreement

Figure 8 Variation of quantity $M\Delta H$ with temperature, for line widths measured in [100] direction.



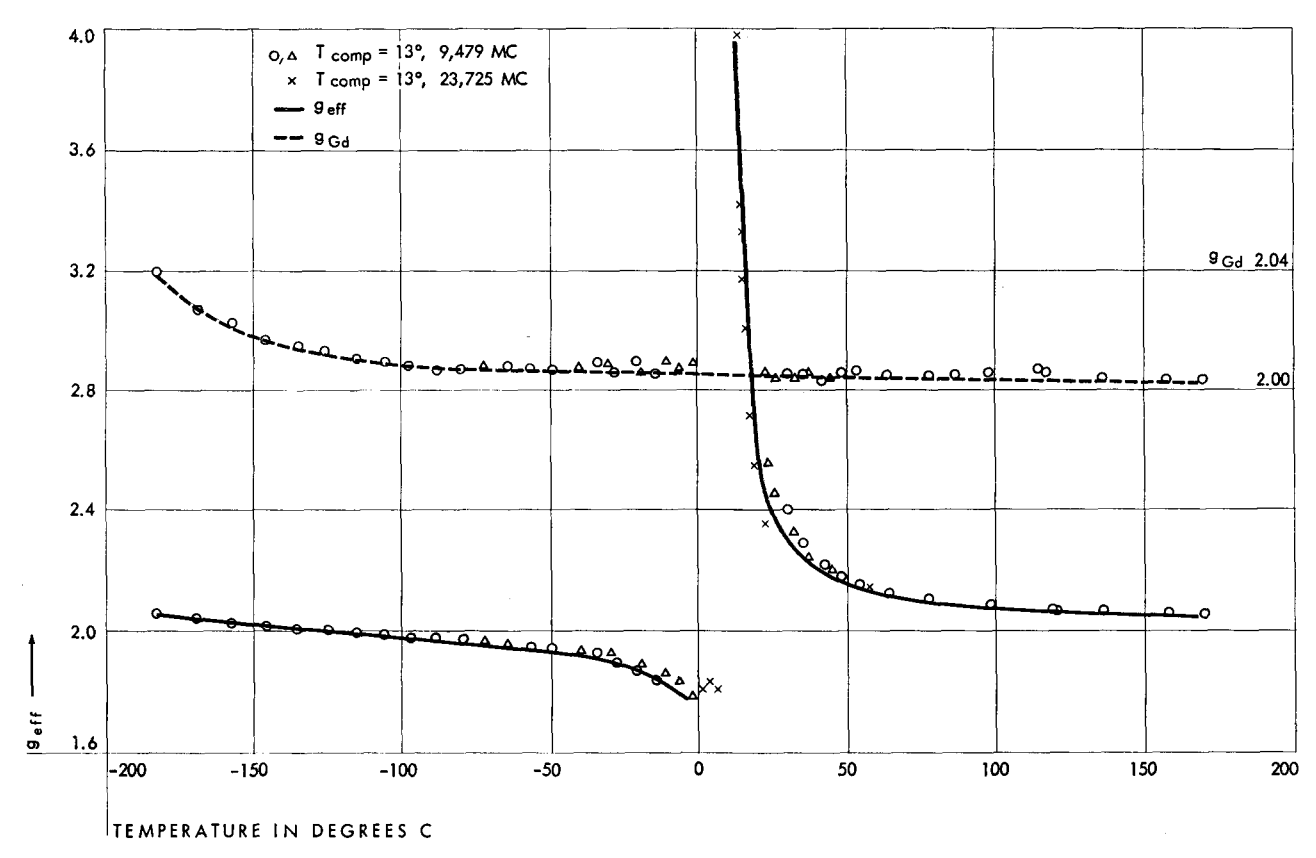
with the value obtained by Geschwind et al¹² at 24,000 Mc. Below -100° C, the observed values of γ_{e} can be fitted only by taking $g_{\rm Gd}$ greater than $g_{\rm Fe}$. The increase in $g_{\rm Gd}$ with decreasing temperature is qualitatively not affected by our assumptions. Measurements on gadolinium garnet crystals grown from a lead oxide flux indicate that $g_{\rm eff}$ and hence $g_{\rm Gd}$ do not increase with decreasing temperature. Until this difference in behavior of the crystals prepared in different ways is clarified, it is premature to speculate on the significance of the apparent temperature dependence of $g_{\rm Gd}$.

We have, until now, neglected the influence of crystalline anisotropy. Since there is no interaction between the damping term and the driving torque $(\mathbf{M} \times \mathbf{H})$ in Eq. (2), we can include the influence of anisotropy in the effective field without modifying our previous discussion of damping. Most discussions of anisotropy near compensation points have been in terms of uniaxial anisotropy. While this form is simpler to handle than cubic anisotropy, only two directions in a cubic crystal, [100] and [111], can be treated in this way. Wangsness19 has obtained a general solution for the resonant frequencies of two coupled sublattices, including the influence of a cubic energy $K_1(\alpha_1^2\alpha_2^2 + \alpha_2^2\alpha_3^2 + \alpha_3^2\alpha_1^2)$ in both sublattices. (Here a_i is the direction cosine of the i^{th} cubic axis with respect to the magnetization). This general solution is extremely cumbersome but the method of simplifying it is well

known. It is expanded in decreasing powers of λM , where λ is the molecular field coefficient describing the interaction between sublattices and M is the resultant magnetization. Except near the compensation point, this quantity is very large and terms involving negative powers of λM are dropped. Under these conditions, one obtains an expression for the resonant field identical with that derived by Kittel²⁰ for ferromagnetic materials except for the replacement of the gyromagnetic ratio with γ_e , given by Eq. (5). Our data for the anisotropy constant determined in this way are shown in Fig. 10. Two things are apparent: (1) the behavior of K_1 in the vicinity of the compensation temperature is very different from the usual monotonic variation with temperature and (2) otherwise, K_1 of gadolinium garnet is the same as that of yttrium garnet above -40° C and becomes more negative at lower temperatures. This second observation suggests that the gadolinium ions do not contribute appreciably to the anisotropy except at low temperature. This is in accord with theoretical expectations.21

To examine the apparent anomaly in the anisotropy around the compensation point, we return to the expansion of the general solution for the resonance field. Algebraic manipulations are considerably simplified by taking the anisotropy associated with the gadolinium sublattice to be zero, as justified above, and by inserting the demagnetizing factors for a spherical sample. Repeating

Figure 9 Measured g_e and calculated g_{Gd} as a function of temperature.



the expansion for the resonant frequency, this time retaining terms involving $(\lambda M)^{-1}$, we obtain

$$\omega^{2} = \gamma_{e}^{2} \left[\left\{ H_{r} + (K_{1}/M)f(\theta) \right\} \left\{ H_{r} + (K_{1}/M)g(\theta) \right\} + \frac{H_{r}^{2}}{\lambda M^{2}} K_{1} \left(f(\theta) + g(\theta) \right) \right],$$

where K_1 is the first-order cubic anisotropy constant and, for a (110) plane with the angle θ measured from the [001] direction to the applied field,

$$f(\theta) = 2 - \sin^2\theta - 3\sin^22\theta$$

and

$$g(\theta) = 2(1-2\sin^2\theta - \frac{3}{8}\sin^2\theta)$$
.

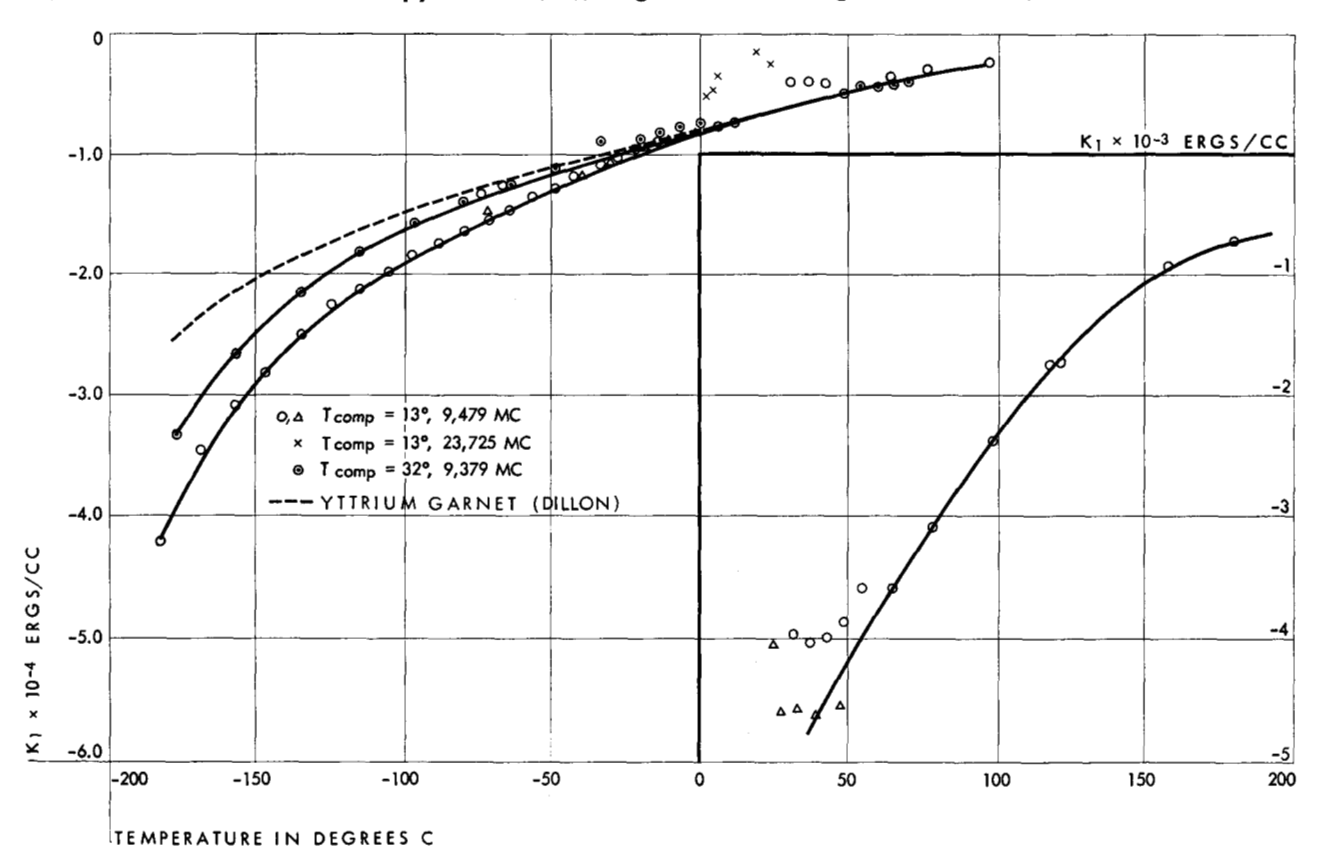
Equation (7) differs from the usual resonance equation only in the inclusion of the last term in the bracket. Unfortunately this equation is not very useful for quantitative calculations. It is extremely cumbersome to manipulate and, even more important, will be a reliable approximation only in a very limited temperature interval. Once the term in $(\lambda M)^{-1}$ becomes important, small changes in temperature will rapidly make the higher-order terms of the series also important. However, inspection of Eq. (7) immediately reveals the cause for the

apparent decrease in K_1 near the compensation temperature. Since both K_1 and λ are negative, the sign of the last term will be positive along the [100] direction and negative along [111]. Hence, the field needed for resonance will be lower in the hard direction and higher in the easy direction than would be the case if the last term were ignored. This effect would be reversed in the anisotropy constant were positive, i.e., the use of the Kittel equation to determine K_1 in such a case would lead to a spurious increase in the anisotropy constant near the compensation point. It should also be noted that this last term in Eq. (7) will alter the expected angular dependence of the resonant field. Deviations from the expected angular dependence of H_r are usually interpreted as evidence of a secondorder anisotropy term. Obviously such a conclusion is questionable in a relatively wide temperature range around a compensation point.

Summary and conclusions

Microwave-resonance absorption in gadolinium-iron garnet has been described in terms of a two-sublattice model, with the assumption that the properties of the iron sublattice are the same as those of yttrium-iron garnet. The data, which do not include the temperature interval within 15° of the compensation point at 13°C, can be satisfactorily treated by the usual theory of resonance of coupled

Figure 10 Variation of anisotropy constant, K1, of gadolinium-iron garnet with temperature.



sublattices, i.e., without explicit consideration of the dependence of the magnetization of the gadolinium lattice on the applied field. Our values for the gyromagnetic ratios of the sublattices, $g_{\rm Gd} = 2.006$ and $g_{\rm Fe} = 2.020$, are in good agreement with the value for $g_{\rm Fe} - g_{\rm Gd}$ determined by Geschwind et al at the compensation temperature. Below $-100^{\circ}{\rm C}$, $g_{\rm Gd}$ increases with decreasing temperature to a value of 2.040 at $-190^{\circ}{\rm C}$.

The anisotropy of gadolinium-iron garnet above -190° C is adequately represented by a first-order term, $K_1(\alpha_1^2\alpha_2^2+\alpha_2^2\alpha_3^2+\alpha_3^2\alpha_1^2)$. The values of a second-order term $K_2(\alpha_1^2\alpha_2^2\alpha_3^2)$ are less than our experimental errors. The inclusion, in the equation for the resonance field, of higher-order terms accounts for the apparent decrease in K_1 near the compensation temperature. In this temperature range, these higher-order terms also influence the angular dependence of the magnetic field required for resonance. The anisotropy constant of gadolinium-iron garnet is equal to that of yttrium garnet above -40° C and becomes more negative at lower temperatures.

The inclusion of damping terms
$$\frac{\alpha}{|\mathbf{M}|} \left(\mathbf{M} \times \frac{d\mathbf{M}}{dt} \right)$$
,

in the equation of motion for the sublattice magnetizations, accounts for the large increase in line width around the compensation temperature. The relative magnitudes of the damping parameters for the sublattices indicate that the gadolinium ions introduce the largest part of the total damping.

Acknowledgments

We are grateful to Dr. S. Geschwind and to Dr. R. K. Wangsness for the privilege of seeing their papers prior to publication. We are indebted to Mr. I. L. Gelles for making his K-band apparatus available to us and for his assistance in obtaining data with it. The x-ray orientation and mounting of the samples were done by Miss H. M. Dunn.

References

- 1. F. Bertaut and F. Forrat, Compt. rend. 242, 382 (1956).
- 2. R. Pauthenet, J. Appl. Phys. 29, 253 (1958).
- S. Geller and M. A. Gilleo, J. Phys. Chem. Solids, 3, 30 (1957).
- 4. J. F. Dillon, Jr., Phys. Rev. 105, 759 (1957).
- Rodrigue, Pippin, Wolf and Hogan, I.R.E. Trans. PGMTT 6, No. 1, 83 (January 1958).
- Le Craw, Spencer and Porter, J. Appl. Phys. 29, 326 (1958) and Abstract Y12, Bulletin of Am. Phys. Soc., 3, 145 (March 1958).
- Calhoun, Overmeyer and Smith, Phys. Rev., 107, 993 (1957).
- 8. J. Pauleve, Compt. rend. 244, 1908 (1957); J. Appl. Phys. 29, 259 (1958).
- Calhoun, Overmeyer and Smith, J. Appl. Phys., 29, 427 (1958).
- L. R. Maxwell and S. J. Pickart, Phys. Rev., 92, 1120 (1953).
- 11. R. L. White and I. H. Solt, Jr., Phys. Rev., 104, 56 (1956).
- S. Geschwind, L. R. Walker and D. F. Linn, Bull. Am. Phys. Soc., Ser. 11, 3, 145 (1958).
- B. Dreyfus, Compt. rend. 241, 552 (1956); 241, 1270 (1956).
- 14. R. K. Wangsness, *Phys. Rev.* **91**, 1085 (1953); **93**, 68 (1954).
- R. K. Wangsness, Bull. Am. Phys. Soc., Ser. 11, 3, 43 (1958); also Phys. Rev. 111, 813 (1958).
- 16. T. Gilbert, Phys. Rev., 100, 1243 (1955).
- 17. Jones, Rodrigue and Wolf, J. Appl. Phys. 29, 434 (1958).
- 18. N. Bloembergen, Proc. I.R.E., 44, 1259 (1956).
- R. K. Wangsness, *Phys. Rev.*, **91**, 1085 (1953). See Eq. 3, p. 1086.
- 20. C. Kittel, Phys. Rev., 73, 155 (1948); 76, 743 (1949).
- 21. W. P. Wolf, Phys. Rev. 108, 1152 (1957).

Revised manuscript received September 30, 1958